

## PREPARATION OF $\gamma$ -ALUMINA FOAMS OF HIGH SURFACE AREA EMPLOYING THE POLYURETHANE SPONGE REPLICA METHOD

A.B. SIFONTES<sup>†</sup>, M. URBINA<sup>†</sup>, F. FAJARDO<sup>†</sup>, L. MELO<sup>†§</sup>, L. GARCÍA<sup>†</sup>, M. MEDIAVILLA<sup>†</sup>, N. CARRIÓN<sup>‡</sup>, J. L. BRITO<sup>§</sup>, P. HERNÁNDEZ<sup>§</sup>, R. SOLANO<sup>\*</sup>, G. MEJIAS<sup>†</sup> and A. QUINTERO<sup>†</sup>

<sup>†</sup> *Facultad de Ingeniería, Universidad Central de Venezuela, UCV, P.O. Box 48.057, Caracas 1041-A, Venezuela*  
e-mail: meloher@gmail.com

<sup>‡</sup> *Centro de Química Analítica, Facultad de Ciencias, Universidad Central de Venezuela, P.O. Box 47102, Caracas 1041-A.*

<sup>§</sup> *Centro de Química, Instituto Venezolano de Investigaciones Científicas, P.O.Box 20632, Caracas 1020-A*

<sup>\*</sup> *Instituto de Superficies y Catálisis " PROF. EDUARDO CHOREN", Facultad de Ingeniería, Universidad del Zulia, LUZ, P.O. Box 15251, Maracaibo, Venezuela*

**Abstract**— Single phase  $\gamma$ -Al<sub>2</sub>O<sub>3</sub> ceramic foams with high surface area (~180 m<sup>2</sup>/g) and porosity (67%) were prepared by the polyurethane sponge method from slurries containing  $\gamma$ -Al<sub>2</sub>O<sub>3</sub> (~40 wt % of solids). Different commercial polyurethane sponges were tested as templates for the ceramic foams, and the better results were obtained with a hydrophilated polyester polyurethane with pore density of 122 ppi, and thermal behavior that suggested the presence of fire retardant and smoke suppressor additives.

The mechanical strength of the ceramic foams depended on several factors, such as the chemical nature of the sponge employed as template, composition of the slurry, and the heating rate during calcination. It was found that at least four cycles of re-coating followed by drying were required before calcination to prevent collapse of the ceramic foams.

**Keywords**—  $\gamma$ -alumina; ceramic foams; polyurethane sponge; textural properties; porous ceramic; X-ray diffraction.

### I. INTRODUCTION

Porous ceramics are finding increasing applications as catalytic supports, ceramics membranes, sensors, filters, thermal and acoustic insulators, due to their properties such as low density, low thermal conductivity, high temperature stability and high resistance to chemical attack (Han *et al.*, 2002, Blachou *et al.*, 1992). The excellent properties of catalysts supports based on porous ceramics has led to the application of this type of catalyst to processes such as hydrotreatment, methanation, fuel cells and biochemical reaction (Irlandoust and Anderson, 1988; Ávila *et al.*, 2005).

Ceramic foams are a special class of porous materials comprised of large voids (cells), with linear dimensions in the range of 10  $\mu$ m to 5 mm and possessing a geometry that, has been approximated to that of a tetra-kaidecahedron (Colombo, 2002).

They are open-cell ceramic structures that may be fabricated in a variety of shapes from a wide range of

materials, and they exhibit very high porosities with good interconnectivity (Twigg and Richardson, 2007). Owing to the combination of their special geometry and resulting properties, they can be used in a wide range of engineering applications.

The most popular manufacturing route for ceramic foams is the polyurethane (PU) sponge replica technique or polymeric sponge method. This methodology allows to obtain open cell porous ceramic structures with a controllable pore size, interconnected pores and desired geometry (Ramay and Zhang, 2003). The first step in the manufacturing route involves dipping a reticulated PU sponge in a ceramic slurry, squeezing out the excess liquid and drying the coated foam. Next, the PU template is burnt out (at around 500 °C) and the structure is sintered at a temperature depending on the desired ceramic material (Blachou *et al.*, 1992, Tripkovic *et al.*, 2006). To deposit the suitable amount of ceramics particles in a single application, the solids content of the slurry has to be high. Alternatively, after a first coating of the support with a less viscous slurry and thermal treatment, several layers of material can be added by additional immersion and thermal treatment cycles. It is important to control the slurry viscosity during the washcoating process, in order to achieve a high loading of ceramic particles, to aid the adhesion of the alumina to the substrate and to prevent the plugging of structure channels (Blachou *et al.*, 1992). The main drawback of ceramic foams produced by this route is their mechanical weakness due to the formation of hollow struts and residual cracks during processing (Han *et al.*, 2002). This limits their performance and their use in certain applications.

The selection of the PU sponge for the preparation of the ceramic foam is an important issue, as the physicochemical properties of these polymers may influence the sinterization of the ceramics during the calcining step. Polyurethane sponge is a cellular solid consisting of areas of PU polymer separated by voids (Parsons and Mountain, 2007). The areas containing solid material are referred to as struts, whilst the voids may be referred to as cells or pores. In mechanical terms, PU sponges

may differ in terms of its density, *i.e.*, mass of struts per unit volume, and porosity, *i.e.*, percentage of pores per unit volume (Parsons and Mountainm, 2007). With regards to their chemical properties, PU sponges may differ due to the various additives that can be incorporated into the polymer mixture, such as flame retardants, blowing agents, anti-oxidants and pigments, which are included in the reaction mixture in order to impart the required characteristics to the final product (Gibson and Ashby, 1999; Parsons and Mountainm, 2007, Saggio-Woyansky *et al.*, 1992). Additionally, PU sponges are generally hydrophobic, lacking good liquid absorption and wicking characteristics, which makes them less suitable for manufacturing absorbent sponges (Herzog and Baatz, 2004). This fact can be a problem, as ceramic slurries employed in the foam replica method are in general water based suspensions. Currently, absorbent sponges are made of polyester- or polyether-polyurethanes. These sponges exhibit hydrophilic properties due to the increased polarity of the carboxylic acid groups (Herzog and Baatz, 2004).

Aluminum oxide or alumina,  $\text{Al}_2\text{O}_3$ , is an important material that can be prepared in several different phases. The most stable form is  $\alpha\text{-Al}_2\text{O}_3$  (Corundum), which is employed as a ceramic material, and is characterized by its high crystallinity and octahedral coordination of aluminum. Other phases of alumina, so-called transition aluminas, are widely used as catalysts, catalytic supports or adsorbents. Among the transition aluminas,  $\gamma\text{-Al}_2\text{O}_3$  is probably the most employed one for applications in catalysis and adsorption, because it can be prepared with high surface area and porosity, has good thermal stability up to 700 °C and useful acid-base surface properties.

Due to the high calcination temperatures employed in the conventional preparation of alumina foams,  $\alpha\text{-Al}_2\text{O}_3$  is always obtained (Han *et al.*, 2002). For catalytic applications, post-treatments such as washcoating of the  $\gamma\text{-Al}_2\text{O}_3$  monoliths with suspensions of  $\gamma\text{-Al}_2\text{O}_3$  or sol-gel deposition procedures can be employed in order to obtain materials with higher surface areas (Twigg and Richardson, 2002). However, when the foam is coated with  $\gamma$ -alumina or any hydrated form of alumina, the maximum useful temperature is limited to approximately 700°C to avoid loss of surface area as the result of the transformation to more crystalline forms of alumina (Han *et al.*, 2003).

To our best knowledge, there has been only one, very recent report on the preparation of single phase  $\gamma\text{-Al}_2\text{O}_3$  ceramic foam (Zhang *et al.*, 2009). The same work also reports the use of these macroporous, monolithic supports for catalytic applications. Another recent article deals with engineering aspects of the use of ceramic foams for gas phase catalytic applications (Zuercher *et al.*, 2009).

In the present work, the preparation of single phase  $\gamma$ -alumina foams of high surface area employing the polyurethane sponge replica technique is reported. Polyurethane sponges with different characteristics and

slurries of two  $\gamma$ -aluminas of varying textural properties were tested for the preparation of the ceramic materials.

## II. METHODS

Three commercial polymeric sponges (“A”, “B”, and “C”) were tested as templates for the preparation of ceramic foams. Sponge “A” corresponds to open cell PU sponge (Marzano Form) with pore density of 5 ppi. (pores per inch). Sponge “B” is an open cell one also made of PU and with pore density of 26 ppi. (Arix Maxi TM). Sponge “C” (ACE Hardware Corp) corresponds to hydrophilated polyester polyurethane with pore density of 122 ppi. The thermal decomposition of the PU sponges was studied by thermogravimetry (TGA): sponge samples were heated from room temperature to 700 °C in a Du Pont 990 Thermogravimetric Analyzer under flow of air (100 mL/min) at a heating rate of 10°C/min.

Two alumina sources were used in the present study for preparing the slurries used in the impregnation process: A commercial  $\gamma$ -alumina with BET surface area of 222 m<sup>2</sup>/g, pore volume of 0.64 cm<sup>3</sup>/g and mean pore radius of 7.8 nm; and a synthesized one prepared in this laboratory following the method reported by Xu *et al.* (2006), and which has 283 m<sup>2</sup>/g BET area, 0.53 cm<sup>3</sup>/g pore volume and mean pore radius of 7.6 nm.

Slurries (with approximately 40 wt% of solids) were prepared using the following procedure: 18 g of pulverized commercial  $\gamma\text{-Al}_2\text{O}_3$  or 21.8 g of the synthesized alumina was mixed with 24 mL of deionized water and 5 mL of concentrated HCl. These weights of either alumina allowed obtaining adequate viscosities of slurries and proper mechanical strengths of the ceramic foams. The resulting slurries were stirred at room temperature for 48 hours at 80-112 rpm. Viscosity measurements of the slurries were carried out with a *Cannon-Fenske* viscometer. The washcoating process comprises the immersion of the sponges in the slurry for 30 s, blowing with air to remove the excess of slurry, and drying at 100 °C for 0.5 h in a convection oven. The dried piece was submitted to a second immersion in the slurry and dried again at 100 °C for 0.5 h, and this immersion-drying treatment was repeated up to four drying cycles. The PU cylinder was compressed before the first immersion and allowed to expand within the slurry in order to infiltrate it. Subsequent immersions were made without compressing the dried piece. Finally, the coated cylinder was calcined at 600°C for 6 h. It was found that a minimum of four immersion-drying cycles were required in order to attain self supporting ceramic cylinders that could withstand the calcination treatments without collapsing. Thus, all the samples prepared were submitted to four impregnation-drying cycles and a final calcinations step. This procedure follows a technique developed previously (Zhu *et al.*, 2001), but in that case each cycle included a calcination step after drying. The dimensions of the resulting cylindrical ceramic pieces were 1.4 cm in diameter and 1.8 cm length.

Different analysis techniques were used to characterize the ceramic samples: X-ray diffraction patterns were collected using a Siemens D-5005 diffractometer, employing CuK $\alpha$  radiation in the  $2\theta$  range between  $5^\circ$  and  $70^\circ$ . The operating voltage and current were 40 kV and 45 mA. Photographs of some samples were taken with a digital camera (Casio, Japan). Scanning Electron Microscopy micrographs were obtained out with a Hitachi S-2400 instrument. The textural properties of the ceramic samples were characterized by N<sub>2</sub> adsorption porosimetry (Micromeritics, ASAP 2010). The samples were first degassed at 300°C under vacuum for more than 24 h until the sample passed the degassing test. Nitrogen adsorption isotherms were measured at liquid N<sub>2</sub> temperature (77 K) and N<sub>2</sub> pressures ranging from 10<sup>-6</sup> to 1.0 P/Po. The BJH method was applied to calculate the pore size distribution.

### A. Results and Discussion

#### *Polyurethane sponge characterization and selection*

Preliminary experiments showed that of the three polymeric sponges tested to prepare ceramic cylinders of  $\gamma$ -alumina, foams prepared with PU sponges "A" and "B" always collapsed upon calcination. On the other hand, pieces made with the PU sponge "C" after proper procedures (see below), kept their cylindrical shapes. In order to understand the different behavior of the polymers, some characterization tests were carried out.

Figure 1 shows the thermal decomposition behavior of 4-mg samples of each of the PU sponges heated at 10°C/min under air flow of 100 mL/min in the TGA equipment at normal pressure. The top panels of Figs. 1a to 1c show plots of the remaining mass of solid ( $m$ ) normalized by the initial sample mass ( $m_0$ ):

$$S_f = m/m_0 \quad (1)$$

where  $S_f$  is the solid mass fraction. The bottom panels of the same figures show the derivative of the solid mass fraction with respect to the temperature ( $dS_f/dT$ ). Thus, figures 1a to 1c show the normalized decomposition plots for the PU sponges. The presence of several steps (top)/peaks or shoulders (bottom) in these curves is indicative that the decomposition of PU sponge is complex and consists of many chemical reactions.

Figures 1a and 1b show similar profiles, decomposition beginning at approximately 240 °C and extending to 380 °C, as clearly observed from the DTG curves. The maximum decomposition rates were observed at about 300-350 °C. In the case of sponge "C", Fig. 1c shows a different shape. The main decomposition occurred between 210 and 590 °C. This sample loses the larger weight percentage (49%) at a temperature of 350°C, corresponding to the maximum rate of decomposition. Furthermore, there are several small peaks and shoulders in the DTG curve of sample "C". These results show that the decomposition behavior of samples "A" and "B" are similar and less complex than that of sample "C", and thus it is likely that the chemical nature of the latter PU sponge is different from that of samples "A" and "B".

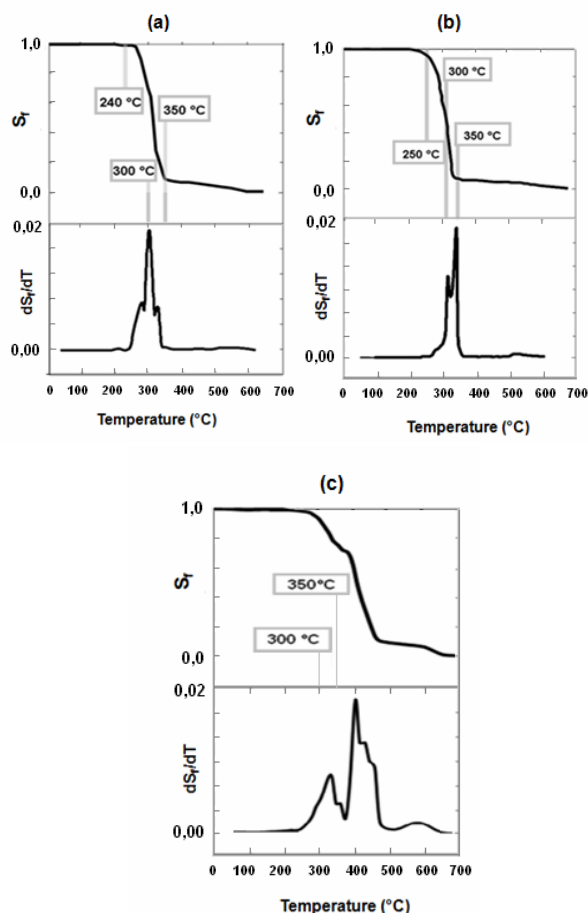


Figure 1. TGA of polyurethane sponges; 10 °C/min; 100 mL/min. air. (a) Sponge "A", 5 ppi.; (b) Sponge "B", 26 ppi.; (c) Sponge "C", 122 ppi.

In a study of the thermal degradation of PU sponges with varying additives, Tang *et al.* (2002) reported three characteristic temperature regions for PU sponge: (1) 120-140 °C, (2) 270-280°C and (3) up to ~480°C. The first region was assigned to evolution of moisture from the sponge, the second to thermal pyrolysis of the polymer, and the third to combustion of the sponge residues (Tang *et al.*, 2002). Dick *et al.* (2001) reported thermal profiles under air showing two regions around 300 and 550 °C, the first one assigned to pyrolysis and the second to combustion of PU. The discrepancies between those results probably stem from the presence of different additives. Thermal degradation of neat PU has been reported to start in the temperature range 110-270°C, while PU materials containing fire retardant additives became degraded at temperatures in excess of 400°C (Chlystek, 1977)

Fire retardant additives (or "Combustion Modifying Additives") added to flexible polyurethane sponge will cause the sponge to be more difficult to ignite, burn less rapidly, or lose less weight during a fire than sponges without additives. Flame retardants are often based on chlorine or bromine compounds, which upon sufficient heating produce chlorine and/or bromine radicals that interfere with the combustion chemistry in the gas phase, resulting in enhanced charring or carbonization.

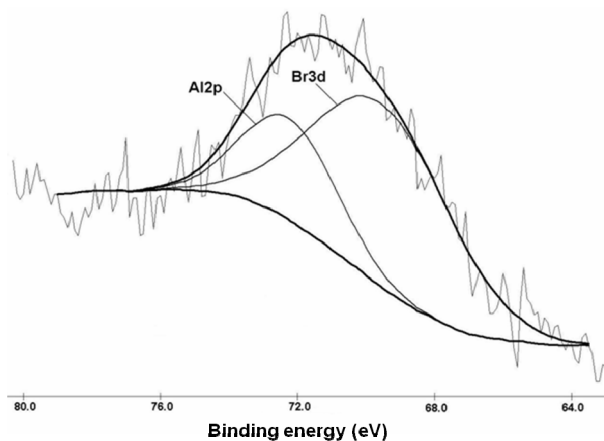


Figure 2. X-ray photoelectron spectra of polyurethane sponge “C” after heating at 400 °C in the region of Al<sub>2p</sub>, Br<sub>3d</sub>.

Halogen presence in the three sponges was checked (Na fusion plus testing with AgNO<sub>3</sub> solution) and only sample “C” gave a positive result. Indeed, XPS measurements in the Al<sub>2p<sub>3/2</sub></sub>-Br<sub>3d<sub>5/2</sub></sub> region of the “C” sponge (Fig. 2) showed low intensity peaks assigned to both these elements, where aluminum could be assigned to another type of additive, *e.g.*, a smoke suppressor based on a metal oxide. None of the metal oxides is an effective flame retardant on its own, but their use in conjunction with halogen compounds often results in systems which are very effective for this role (Hirschler, 1984).

On the other hand, the reported composition of the PU “C” corresponds to hydrophilated polyester polyurethane, whose hydrophilic characteristics could help to absorb more efficiently the aqueous slurry of alumina into the sponge pores.

In the second stage of weight loss of sponge “C”, related to PU combustion, it occurs the oxidation of the carbonaceous skeleton which remains after the initial decomposition. This can be appreciated by comparing Figs. 3 and 4 that show micrographies of “C” sponge before (Fig. 3) and after (Fig. 4) calcination in a muffle furnace at 400 °C. As can be seen in Fig. 4, the carbonaceous skeleton is preserved and shows morphology similar to the starting PU pore system. It has been shown that the rate of oxidation is dependent on the heating rate. At slow heating rates (2.5 °C/min or slower) a more porous carbon skeleton is formed, allowing oxidation to proceed at a higher velocity. Faster heating rates would produce less porous carbon skeletons, resulting in slower oxidation rates (Kirk-Othmer, 2001, Luda *et al.*, 2004). In the cases of sponges “A” and “B”, calcination at 400°C produced powdered ashes with no cellular structure independently of the heating rate.

Thus, PU sponge “C” was selected for all the preparations. An additional consideration is that generally the polymeric sponge decomposes and gives out large amounts of gas during the firing process. The removal of the polymeric skeleton and the impact of the large volumes of gas, produce defects and cracks in the structure of the ceramics foams, which leads to collapse.

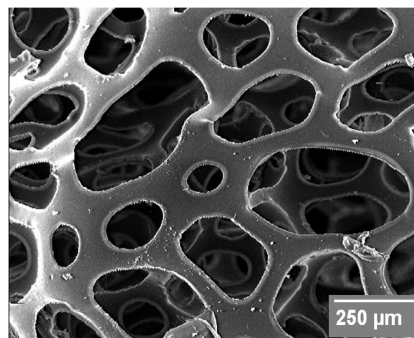


Figure 3. SEM of polyurethane sponge “C”.

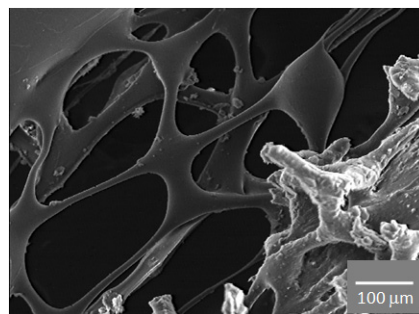


Figure 4. SEM of polyurethane sponge “C” after heating in air at 400 °C.

Control of the heating rate is thus an important factor to avoid collapse during calcination. Slow heating is also needed for reducing the rate of gas evolution and to maintain the pore structure. In the present work, a heating rate of 1°C/min was chosen for heat treatment (calcination) of the ceramic foams obtained from PU “C”, a condition that prevents the collapse of the ceramics pieces upon firing.

#### Preparation of $\gamma$ -alumina foams

The alumina coating was applied by repeated immersion-drying cycles of the substrate (PU sponge “C”) in one of the alumina slurries. The viscosity of the slurry prepared with commercial  $\gamma$ -alumina at pH 3.5 was  $65 \times 10^{-4}$  Pa.s; for the slurry prepared with the synthesized alumina, it was  $103 \times 10^{-4}$  Pa.s. These viscosity values are within the expected range, according to previous literature reports (Blachou *et al.*, 1992).

The PU support coated with the wet slurry was blown with air to remove excess slurry and subsequently dried at about 100°C. After the fourth coating/drying cycle, it was calcined. In order to choose the conditions for the firing step, PU sponges were tested employing TGA, as described above, in order to determine the temperature range through which slow heating is needed.

The PU sponge “C” impregnated with the slurries was heated at the rate of 1°C/min between 25 and 600°C and kept at this final temperature for 6 h, without collapse of the resulting ceramic foams. Figure 5 shows a photograph of a typical alumina ceramic foam sample obtained by application of the indicated preparation methods, employing the alumina sample synthesized in the laboratory.

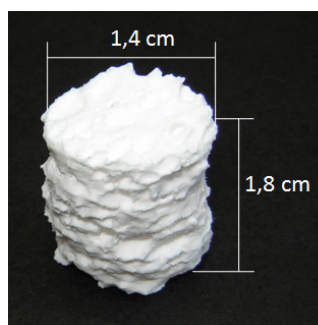


Figure 5. Photographs of  $\gamma$ -alumina foams prepared from polyurethane "C" and synthesized  $\gamma$ -alumina.

#### Mechanical strength of the ceramic foams

Calcined alumina foams showed mechanical strength (resistance to breakup/crushing) of the order of 100 kPa for the samples obtained from the commercial alumina and 315 kPa for those produced from the synthesized alumina. While these mechanical strength values are not particularly high if compared with data reported for  $\alpha$ -alumina foams, it must be taken into account that the present ceramic materials are calcined at relatively low temperatures in order to keep the alumina in the  $\gamma$ -phase, which is the interesting one from the catalysis/adsorption point of view. For the sake of comparison, Han *et al.* (2002), reported mechanical strengths in the range between 275 kPa and 1.3 Mpa for  $\alpha$ -alumina foams showing BET areas close to  $4 \text{ m}^2/\text{g}$ .

The observed differences in mechanical properties could be assigned to a lower particle size of the synthesized alumina (hence the higher surface area), allowing the preparation of more viscous slurries that permit a better impregnation of the PU template with the alumina solids. The thickness of the covering layers on the polymeric sponges depends on the viscosity of the slurry. It was found experimentally that slurries with viscosities above  $130 \times 10^{-4} \text{ Pa}\cdot\text{s}$  tend to produce thicker layers with tendency to break during the drying stage.

#### Textural properties of $\gamma\text{-Al}_2\text{O}_3$ ceramic foams

The initial aluminas keep their crystalline properties after preparation of the ceramic structures as shown by the XRD patterns (Fig. 6), which present three main peaks placed at  $d$ -spacings of 0.239, 0.197, and 0.139 nm, corresponding respectively to the  $d_{311}$ ,  $d_{400}$ ,  $d_{440}$  reflections of the  $\gamma\text{-Al}_2\text{O}_3$  phase (Xu *et al.*, 2006).

However, the intensity of the peaks decrease when passing from the alumina precursors (Fig. 6-a, and 6-c) to the ceramic foams (Fig. 6-b, and 6-d), and this effect is more pronounced for the commercial precursor.

Table 1 collects the results of textural characterization of the prepared solids. It reports the BET surface area, total pore volume obtained from the  $\text{N}_2$  physisorption isotherm at 0.99 relative pressure, and mean pore radius (from BJH method). The ceramic foams, as well as the initial aluminas, are characterized by a low micropore volume (below  $0.01 \text{ cm}^3/\text{g}$ , calculated from t-plot method) and mean pore radius in the range of mesopores.

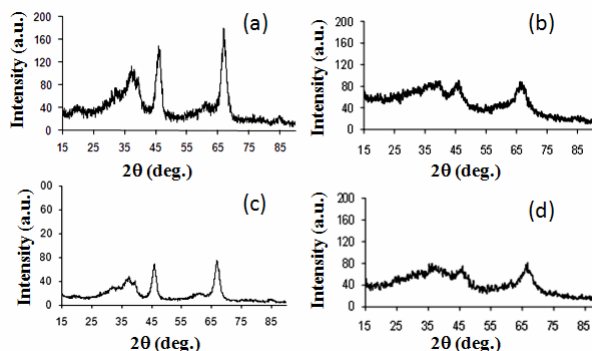


Figure 6. XRD patterns of: (a) commercial  $\gamma$ -alumina; (b)  $\gamma$ -alumina ceramic foam prepared from commercial alumina; (c) synthesized  $\gamma$ -alumina; (d)  $\gamma$ -alumina ceramic foam prepared from synthesized alumina.

Table 1. Textural properties of  $\gamma$ -alumina ceramic foams and of alumina precursors.

Sample	$S_{\text{BET}}$ ( $\text{m}^2\text{g}^{-1}$ )	$V_{\text{por}}$ ( $\text{cm}^3\text{g}^{-1}$ )	$D_p$ (nm)
Commercial $\gamma\text{-Al}_2\text{O}_3$	222	0.64	7.8
Synthesized $\gamma\text{-Al}_2\text{O}_3$	283	0.53	7.6
Commercial $\gamma\text{-Al}_2\text{O}_3$ ceramic foam	178	0.57	10.1
Synthesized $\gamma\text{-Al}_2\text{O}_3$ ceramic foam	179	0.48	9.8

$S_{\text{BET}}$ : Total Surface Area (BET)

$V_{\text{por}}$ : Pore volume

$D_p$ : Pore diameter ( $D_{\text{BJH}}$ )

Figures 7-a, 7-c, 8-a, and 8-c show the  $\text{N}_2$  physisorption isotherms of the commercial and synthesized  $\gamma\text{-Al}_2\text{O}_3$  and of the ceramic foams prepared from these precursors. The shapes of the isotherms correspond to type IV of the BET classification, characteristic of mesoporous materials (Gregg and Sing, 1982).

The pore size distribution curves were derived from the  $\text{N}_2$  physisorption isotherms according to the BJH method, Figs. 7-b, 8-b, 7-d, and 8-d show, respectively, the pore size distributions for the commercial and synthetic  $\gamma\text{-Al}_2\text{O}_3$ ; and the ceramic foams obtained from the same aluminas. The trends are similar in both cases, *i.e.*, the ceramic foams show broader pore size distributions than the parent aluminas. The commercial alumina shows a distribution centered at 7.8 nm, while the foam prepared from this material shows a maximum around the same value, but also a shoulder at higher pore diameter. The synthesized alumina is characterized by a narrower distribution centered around 7.6 nm. The foam prepared from this alumina shows a bimodal distribution, with a maximum of low intensity at 6.5 nm and a second higher intensity maximum at about 9.8 nm.

The porosities of the fired products were calculated by means of the equation (Park *et al.*, 2005):

$$\text{Porosity} = (\rho_r - \rho_b) / \rho_r \quad (2)$$

where  $\rho_r$  and  $\rho_b$  are the real and bulk densities, respectively. For the cylindrical structures, the bulk densities were simply calculated from their weight and geometric volumes. As for the real densities, the cylinders were first ground to powder and then measured with a pycnometer. The average porosity of the alumina foams was close to 67 %.

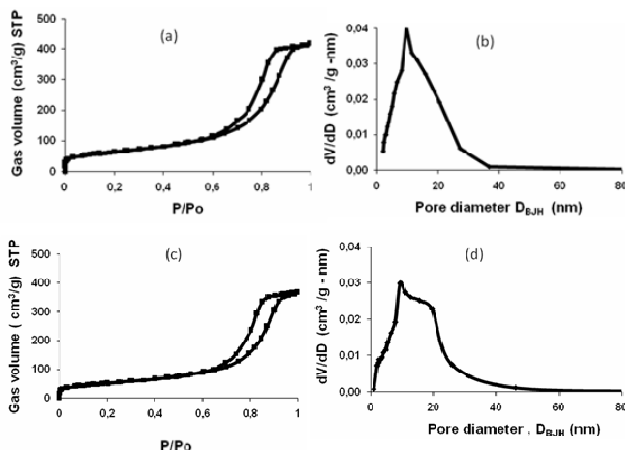


Figure 7. (a)  $N_2$  physisorption isotherm of commercial  $\gamma$ -alumina; (b) Pore size distribution of commercial  $\gamma$ -alumina; (c)  $N_2$  physisorption isotherm of commercial  $\gamma$ -alumina ceramic foam; (d) Pore size distribution of commercial  $\gamma$ -alumina ceramic foam.

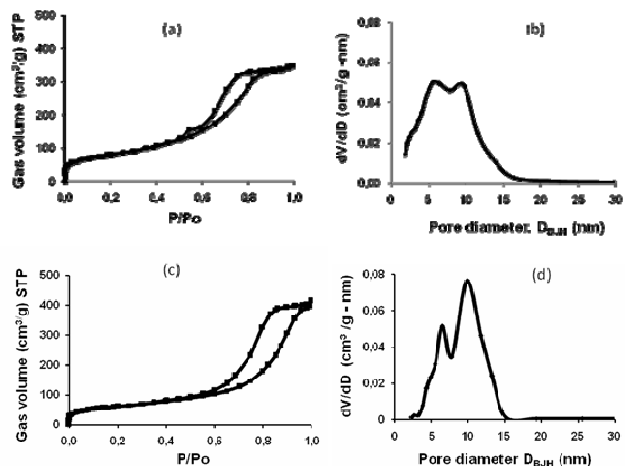


Figure 8. (a)  $N_2$  physisorption isotherm of synthesized  $\gamma$ -alumina; (b) Pore size distribution of synthesized  $\gamma$ -alumina; (c)  $N_2$  physisorption isotherm of synthesized  $\gamma$ -alumina ceramic foam; (d) Pore size distribution of synthesized  $\gamma$ -alumina ceramic foam.

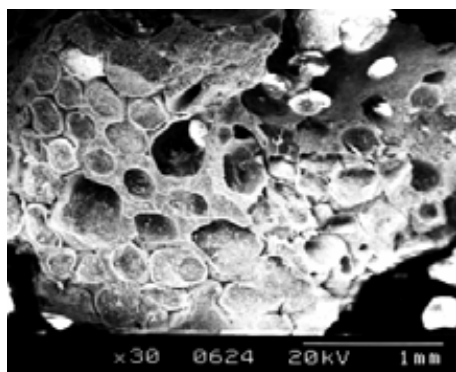


Figure 9. SEM micrographs of  $\gamma$ -alumina ceramic foam prepared from polyurethane sponge "C" and synthesized  $\gamma$ -alumina.

#### Morphology of $\gamma$ -alumina ceramic foams

Figure 9 shows a micrograph of the ceramic alumina foam obtained employing sponge "C" and the synthe-

sized  $\gamma$ -alumina, where it can be appreciated the presence of regular shaped pores (between 0.3 and 0.5 mm) with some smooth surfaces and channels. From the comparison of Figs. 9 and 3, the template effect of the PU sponge procedure is evident.

The combined results of the present study demonstrate the feasibility of producing  $\gamma$ - $Al_2O_3$  ceramic foams with high surface areas and porosities, showing relatively good mechanical strength, which could have potential interest for applications in adsorption and catalysis.

### III. CONCLUSIONS

The synthesis method employed in the present work allowed to obtain  $\gamma$ - $Al_2O_3$  ceramic foams of high surface area ( $\sim 180$   $m^2/g$ ) and porosity (67%). The mechanical strength of the ceramic foams depends on the composition of the slurry, nature of the sponge used as template (*i.e.*, hydrophilicity, presence of additives), heating rate during calcination, and the need of several cycles of re-coating before calcination. The phase composition and structural properties of the aluminas employed were not changed after its use in the preparation of the alumina foams.

### ACKNOWLEDGMENTS

The authors would like to thank CDCH-UCV (PG-O8-00-6075 2005) for supporting this work.

### REFERENCES

- Ávila, P., M. Montes and E.E. Miro, "Monolithic reactors for environmental applications: A review on preparation technologies," *Chem. Eng. J.*, **109**, 11-36 (2005).
- Blachou, V., D. Goula and C. Philippopoulos, "Wet milling of alumina and preparation of slurries for monolithic structures impregnation," *Ind. Eng. Chem. Res.*, **31**, 364-369 (1992).
- Colombo, P., "Ceramic foams: fabrication, properties and applications," *Key Eng. Mater.*, **206-213**, 1913-1918 (2002).
- Chlystek S.J., *Low-smoke generating polyurethane foam*, U. S. Patent No. 4053439 (1977).
- Dick, C., E. Dominguez-Rosado, B. Eling, J.J. Liggat, C.I. Lindsay, S.C. Martin, M.H. Mohammed, G. Seeley and C.E. Snape, "The flammability of urethane-modified polyisocyanurates and its relationship to thermal degradation chemistry," *Polymer*, **42**, 913-923 (2001).
- Gibson, L.J. and M.F. Ashby, *Cellular Solids: Structure and Properties*, Cambridge University Press, Cambridge, U.K. (1999).
- Gregg, S.J. and K.S. Sing, *Adsorption, Surface Area and Porosity*, 2nd Ed., London. Academic Press. (1982).
- Han, Y.S., J.B. Li, Y.J. Chen and Q.M. Wei, "A study on the factors involved in collapse of macroporous  $\alpha$ - $Al_2O_3$  structure," *J. Mater. Proc. Technol.*, **128**, 313-317 (2002).

- Han, Y.S., J.B. Li and Y.J. Chen, "Fabrication of bimodal porous alumina ceramics," *Mater. Res. Bull.*, **38**, 373-379 (2003).
- Herzog, K.P. and G. Baatz, *Composites comprising a hydrophilic polyester-polyurethane foamed material for vehicle interior trim*, U.S. Patent No. 6673849 (2004).
- Hirschler, M.M., "Reduction of smoke formation from and flammability of thermoplastic polymers by metal oxides," *Polymer*, **25**, 405-411 (1984).
- Irandoust, S. and B. Andersson, "Monolithic catalysts for non-automobile applications," *Catal. Rev.-Sci. Eng.*, **30**, 341-392 (1988).
- Kirk-Othmer, *Encyclopedia of Chemical Technology*, Wiley-InterScience (2001).
- Luda, M.P., P. Bracco, L. Costa and S.V. Levchik, "Discolouration in fire retardant flexible polyurethane foams. Part I. Characterisation," *Polym. Degr. Stab.*, **83**, 215-220 (2004).
- Park, H.C., Y.B. Lee, S.G. Lee, C.H. Lee, J.K. Kim, S.S. Hong and S.S. Park, "Synthesis of beta-alumina powders by microwave heating from solution-derived precipitates," *Ceram. Int.*, **31**, 293-296 (2005).
- Parsons, N.S. and C.A. Mountainm, "Investigating polyurethane foam as a form of trace evidence," *Science and justice*, **47**, 24-33 (2007).
- Ramay, H.R. and M. Zhang, "Preparation of Porous Hydroxyapatite Scaffolds by Combination of the Gel-casting and Polymer Sponge Methods," *Bio-materials*, **24**, 3293-3302 (2003).
- Saggio-Woyansky, J., C.E. Scott and W.P. Minnaer, "Processing of porous ceramics," *Am. Ceram. Soc. Bull.*, **71**, 1674-1682 (1992).
- Tang, Z., M.M. Maroto-Valer, J.M. Andrésen, J.W. Miller, M.L. Listemann, P.L. McDaniel, D.K. Morita and W.R. Furlan, "Thermal degradation behavior of rigid polyurethane foams prepared with different fire retardant concentrations and blowing agents," *Polymer*, **43**, 6471-6479 (2002).
- Twigg, M.V. and J.T. Richardson, "Theory and applications of ceramic foam," *Chem. Eng. Res. Des.*, **80**, 183-189 (2002).
- Twigg, M.V. and J.T. Richardson, "Fundamentals and applications of structured ceramic foam catalysts," *Ind. Eng. Chem. Res.*, **46**, 4166-4177 (2007).
- Tripkovic, D., V. Radojevic and R. Aleksic, "Factors affecting the microstructure of porous ceramics," *J. Serb. Chem Soc.*, **71**, 277-284 (2006).
- Xu, B.J, T.C. Xiao, Z.F. Yan, X. Sun, J. Sloan, S.L. González-Cortés, F. Alshahrani and M.L.H. Green, "Synthesis of mesoporous alumina with highly thermal stability using glucose template in aqueous system," *Microp. Mesop. Mat.*, **91**, 293-295 (2006).
- Zhang, Y., C.Y. Zhao, H. Liang and Y. Liu, "Macroporous Monolithic Pt/ $\gamma$ -Al<sub>2</sub>O<sub>3</sub> and K-Pt/ $\gamma$ -Al<sub>2</sub>O<sub>3</sub> Catalysts Used for Preferential Oxidation of CO," *Catal. Lett.*, **127**, 339-347 (2009).
- Zhu, X.W., D.G. Jiang, S.H. Tan and Z.Q. Zhang, "Improvement in the Strut Thickness of Reticulated Porous Ceramics," *J. Am. Ceram. Soc.*, **84**, 1654-1656 (2001).
- Zuercher, S., K. Pabst and G. Schaub, "Ceramic foams as structured catalyst inserts in gas-particle filters for gas reactions. Effect of backmixing," *Appl. Catal. A: Gen.*, **357**, 85-92 (2009).

Received: May 25, 2009.

Accepted: July 20, 2009.

Recommended by Subject Editor Ricardo Gómez.